Journal of Molecular Spectroscopy 319 (2016) 17–25

Contents lists available at ScienceDirect

Journal of Molecular Spectroscopy

journal homepage: www.elsevier.com/locate/jms

High resolution FTIR study of $^{34}S^{16}O_2$: Re-analysis of the bands $\nu_1 + \nu_2$, $\nu_2 + \nu_3$, and first analysis of the hot band $2\nu_2 + \nu_3 - \nu_2$

O.N. Ulenikov [a,*], E.S. Bekhtereva [a], O.V. Gromova [a], T. Buttersack [b], C. Sydow [b], S. Bauerecker [b]

[a] Institute of Physics and Technology, National Research Tomsk Polytechnic University, Tomsk 634050, Russia
[b] Institut für Physikalische und Theoretische Chemie, Technische Universität Braunschweig, D-38106 Braunschweig, Germany

ARTICLE INFO

Article history:
Received 3 October 2015
In revised form 21 November 2015
Accepted 24 November 2015
Available online 2 December 2015

Keywords:
$^{34}SO_2$ sulfur dioxide
High-resolution spectra
Spectroscopic parameters

ABSTRACT

The high resolution infrared spectrum of the $^{34}S^{16}O_2$ molecule was re-investigated in the region of 1600–1900 cm^{-1}. The earlier studied by Lafferty et al., the $\nu_2 + \nu_3$ band was re-analyzed under consideration of transitions with higher values of quantum numbers J and K_a. The weak $\nu_1 + \nu_2$ cold band and the $2\nu_2 + \nu_3 - \nu_2$ hot band were analyzed for the first time. The obtained experimental data were used in the weighted fit procedure based on the effective Hamiltonian which takes into account resonance interactions between a variety of vibrational states. The obtained set of spectroscopic parameters reproduces the initial experimental data with accuracies close to experimental uncertainties.

1. Introduction

Sulfur dioxide is an important species in many fields of research, such as chemistry, interstellar space, planetary nebulae, study of atmospheres of the Earth and Venus, food technology, and many others (see, e.g., Refs. [1–9]). For this reason the high resolution spectra of sulfur dioxide have been subject of extensive laboratory investigations during a long time both in the microwave and infrared (IR) spectral regions (see, e.g., review in Ref. [10]). In the present study we discuss the high resolution spectrum of $^{34}S^{16}O_2$, which is the naturally most abundant (relative band strengths for the $^{34}S^{16}O_2$ and $^{32}S^{16}O_2$ species in natural abundance is about 1:24) and studied species after $^{32}S^{16}O_2$, and focus on the region of 1600–1900 cm^{-1} where the $\nu_1 + \nu_2$ and $\nu_2 + \nu_3$ bands are located.

In the preceding spectroscopic studies of the sulfur dioxide molecule in the gas phase, the region of 1600–1900 cm^{-1} and the rotational structures of the vibrational states (1 1 0) and (0 1 1) have been discussed in Refs. [11–16]. The spectra of the $^{34}S^{16}O_2$ molecule have been analyzed earlier in Refs. [12–14,17–27]. However, the $\nu_1 + \nu_2$ and $\nu_2 + \nu_3$ bands of $^{34}S^{16}O_2$ have been considered in Ref. [14] only (see statistical information in Table 1). An experimental study of the hot band $2\nu_2 + \nu_3 - \nu_2$ and the vibrational state (021) was not mentioned earlier. Here, the experimental spectrum of $^{34}S^{16}O_2$ was recorded in the region of 1050–2050 cm^{-1} in the infrared laboratory of the Technische Universität Braunschweig (Germany), and corresponding experimental details are presented in Section 2. Section 3 briefly gives the theoretical background for the description of the experimental data. The results of the analysis of the experimental data are discussed in Section 4.

2. Experimental details

As described in detail in our preceding papers [28,29] and especially [25,26] the $^{32}SO_2$ sample was generated by controlled combustion of ^{34}S which was purchased from Sigma–Aldrich with a purity of 90 atom%. Two spectra of the spectral region between 1200 and 2800 cm^{-1} have been recorded with a Bruker IFS120HR Fourier transform infrared spectrometer in a one-meter based White cell made from stainless steel at 24 m pathlength each with different optical filters and then exploited for the theoretical analysis. A globar radiation source and KBr windows have been used for both spectra; a KBr beamsplitter and a mercury–cadmium–telluride (MCT) semiconductor detector for the first spectrum (1200–2000 cm^{-1}, compare Figs. 1 and 2), and a CaF2 beamsplitter as well as an indium–antimonide (InSb) semiconductor detector for the second spectrum (1800–2800 cm^{-1}). The transmission spectrum was obtained by division of the highly resolved single-channel spectrum by a background spectrum with a lower resolution of 0.1 cm^{-1} (averaged by 200 scans). The optical resolution was 0.0021 cm^{-1} and 0.0025 cm^{-1} for the first and the second spectrum, defined by $1/d_{MOPD}$ (maximum optical path difference). In combination with the weak Norton–Beer apodization this leads to an instrumental resolution between 0.0017 and 0.0020 cm^{-1}

* Corresponding author.
E-mail address: Ulenikov@mail.ru (O.N. Ulenikov).

http://dx.doi.org/10.1016/j.jms.2015.11.003
0022-2852/

Table 1
Statistical information for the $\nu_1+\nu_2$, $\nu_2+\nu_3$, and $2\nu_2+\nu_3-\nu_2$ bands of $^{34}S^{16}O_2$.

Band	Center (cm^{-1})	J^{max}	K_a^{max}	N_{tr}[a]	N_l[b]	m_1[c]	m_2[c]	m_3[c]
1	2	3	4	5	6	7	8	9
$\nu_1+\nu_2$, Ref. [14]	1654.8290	42	16		349	69.0	24.7	10.3
$\nu_1+\nu_2$, This work	1654.8300	65	23	1540	707	70.3	23.3	6.4
$\nu_2+\nu_3$, Ref. [14]	1854.6105	57	19		608	66.3	24.9	8.8
$\nu_2+\nu_3$, This work	1854.6114	67	23	1390	740	77.8	13.3	8.9
$2\nu_2+\nu_3-\nu_2$, This work	1849.9662	44	15	510	304	57.4	25.1	17.5

[a] N_{tr} is the number of assigned transitions.
[b] N_l is the number of obtained upper-state energies.
[c] Here $m_i = n_i/N_l \times 100$ % (i = 1, 2, 3); n_1, n_2, and n_3 are the numbers of upper-state energies for which the differences $\delta = E^{exp} - E^{calc}$ satisfy the conditions $\delta \leqslant 2\times10^{-4}$ cm^{-1}, 2×10^{-4} $cm^{-1} < \delta \leqslant 4\times10^{-4}$ cm^{-1}, and $\delta > 4\times10^{-4}$ cm^{-1}.

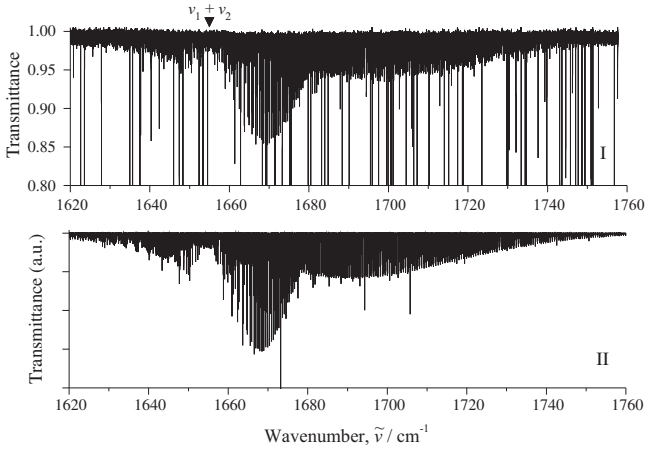

Fig. 1. Survey spectrum (upper trace I) of $^{34}S^{16}O_2$ in the region of the $\nu_1+\nu_2$ band. Experimental conditions: sample pressure is 240 Pa, absorption path length is 24 m; room temperature; number of scans is 840. The lower trace (II) is the simulation spectrum (see text for details of simulation).

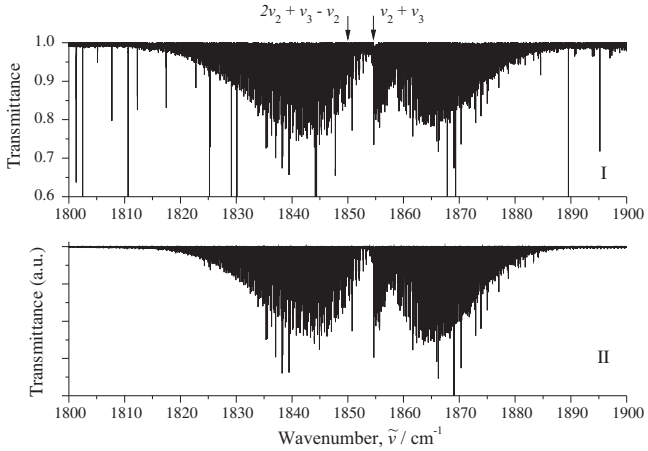

Fig. 2. Survey spectrum (upper trace I) of $^{34}S^{16}O_2$ in the region of the $\nu_2+\nu_3$ band. For the experimental conditions see caption of Fig. 1. The lower trace (II) is the simulation spectrum (calculations of relative line strengths were made with only one, the main, dipole moment parameter and Doppler profile of the lines).

in the 1550–1900 cm^{-1} range which is important for the present work. The Doppler broadening for $^{34}S^{16}O_2$ at 298.15 K was between 0.0024 cm^{-1} (at 1550 cm^{-1}) and 0.0029 cm^{-1} (at 1900 cm^{-1}). The pressure broadening was between 0.0008 and 0.0016 cm^{-1} at the used pressure of 240 and 480 Pa which means that it has to be considered, at least in the 480 Pa case. So the total line widths result between 0.0027 and 0.0036 cm^{-1} (root sum square approximation of convolution) in accordance with the experimental results. The spectral line calibration was performed with N_2O lines at a partial N_2O pressure of about 10 Pa and with water lines, Ref. [30]. The total recording time was 40 and 34 h for 840 scans (0.0021 cm^{-1} resolution, 240 Pa, first spectrum) and 810 scans (0.0025 cm^{-1} resolution, 480 Pa, second spectrum). The recording time was high enough for little amounts of water pouring into the White cell during measurement. In contrast, in the spectrometer nearly no water is present during recording of spectra as it is continuously pumped by a turbo molecular pump below 10^{-2} Pa. The strong extraneous lines in the experimental spectra shown in Figs. 1 and 2 arise from water vapor outgassing in the White cell during the long recording time.

3. Theoretical background

Following the strategy of our preceding papers [25,26], in the theoretical analysis of the experimental data we used the effective Hamiltonian model. For the values of quantum number K_a between 12 and 14 this model takes strong local resonance interactions between the ro-vibrational states $[JK_aK_c]$ of $(\nu_1\nu_2\nu_3)$ and the states $[JK_a \pm 2K_c \mp 2]$ of $(\nu_1 \pm 1\nu_2 \mp 2\nu_3)$ into account (see, e.g., Refs. [20,31]). This means that the Fermi type interaction between the vibrational state (110), analyzed in the present study, and the state (030) should be considered. Analogously, Fermi interaction between the states (021) and (101) should be also considered. In the same way as in [25,26], we found for the description of our experimental data, that the Coriolis type resonance interactions can be neglected. The effective Hamiltonian model which was used in the present study has the form (see, e.g., Refs.[32–34]):

$$H^{\text{vib.-rot.}} = \sum_{v,\tilde{v}} |v\rangle\langle\tilde{v}| H^{v\tilde{v}}, \tag{1}$$

where v and $\tilde{v}$ denote interacting vibrational states, and the summation extends over five vibrational states: $|1\rangle \equiv (110, A_1)$, $|2\rangle \equiv (030, A_1)$, $|3\rangle \equiv (011, B_1)$, $|4\rangle \equiv (021, B_1)$, and $|5\rangle \equiv (101, B_1)$. In this case, Fermi interactions take place only between the pairs of vibrational states (110)/(030) and (101)/(021); the state (011) is considered as isolated. The operators in the diagonal blocks of Eq. (1) are the Watson type operators in the A reduction and I^r representation, [35–37],

$$\begin{aligned} H^{vv} = {} & E^v + \left[A^v - \frac{1}{2}(B^v + C^v)\right]J_z^2 + \frac{1}{2}(B^v + C^v)J^2 + \frac{1}{2}(B^v - C^v)J_{xy}^2 \\ & - \Delta_K^v J_z^4 - \Delta_{JK}^v J_z^2 J^2 - \Delta_J^v J^4 - \delta_K^v [J_z^2, J_{xy}^2]_+ - 2\delta_J^v J^2 J_{xy}^2 + H_K^v J_z^6 \\ & + H_{KJ}^v J_z^4 J^2 + H_{JK}^v J_z^2 J^4 + H_J^v J^6 + [h_K^v J_z^4 + h_{JK}^v J_z^2 J^2 + h_J^v J^4, J_{xy}^2]_+ \\ & + L_K^v J_z^8 + L_{KKJ}^v J_z^6 J^2 + L_{JK}^v J_z^4 J^4 + L_{JJK}^v J_z^2 J^6 + L_J^v J^8 \\ & + [l_K^v J_z^6 + l_{KJ}^v J_z^4 J^2 + l_{JK}^v J_z^2 J^4 + l_J^v J^6, J_{xy}^2]_+ + P_K^v J_z^{10} + P_{KKKJ}^v J_z^8 J^2 \\ & + P_{KKJ}^v J_z^6 J^4 + \cdots \end{aligned} \tag{2}$$

In Eq. (2), J_α ($\alpha = x, y, z$) are the components of the angular momentum operator defined in the molecule-fixed coordinate system, $J_{xy}^2 = J_x^2 - J_y^2$, and $[\ldots,\ldots]_+$ denote anticommutators. The nondiagonal block operators describe the Fermi interactions and have the following form, Refs. [38,39]:

$$\begin{aligned} H^{v\tilde{v}} = {} & {}^{v\tilde{v}}F_0 + {}^{v\tilde{v}}F_K J_z^2 + {}^{v\tilde{v}}F_J J^2 + {}^{v\tilde{v}}F_{KK} J_z^4 + {}^{v\tilde{v}}F_{KJ} J_z^2 J^2 + {}^{v\tilde{v}}F_{JJ} J^4 \\ & + \cdots + {}^{v\tilde{v}}F_{xy}(J_x^2 - J_y^2) + {}^{v\tilde{v}}F_{Kxy}\{J_z^2, (J_x^2 - J_y^2)\}_+ \\ & + 2\,{}^{v\tilde{v}}F_{Jxy} J^2 (J_x^2 - J_y^2) + {}^{v\tilde{v}}F_{KKxy}\{J_z^4, (J_x^2 - J_y^2)\}_+ + \cdots \end{aligned} \tag{3}$$

4. Assignment of transitions and analysis of the results

To give the reader an impression about the experimental result, the survey spectra of the $\nu_1+\nu_2$ and $\nu_2+\nu_3$ bands are shown in the upper traces of Figs. 1 and 2. Small parts of the high resolution spectra of the $\nu_1+\nu_2$ and $\nu_2+\nu_3$ bands are presented in the upper traces of Figs. 3 and 4.

The $^{34}S^{16}O_2$ molecule is an asymmetric top molecule with the parameter of asymmetry $\kappa=(2B-A-C)/(A-C)\simeq-0.939$, its vibrational modes q_1 and q_2 are symmetric, and the third vibrational mode, q_3, is antisymmetric. In consequence, the (011) and (021) vibrational state, which are considered in the present study, are antisymmetric, and corresponding $\nu_2+\nu_3$ and $2\nu_2+\nu_3-\nu_2$ bands are of *a*-type (see, e.g., Refs. [40–42]). For bands of such type the selection rules are:

$$\Delta J=0,\ \pm1,\quad \Delta K_a=\text{even},\quad \Delta K_c=\text{odd}.$$

It is necessary also to take into account that, due to nuclear spin statistics, only ro-vibrational states with even values of $(K'_a+K'_c)$ are allowed for vibrational states of the A_1 symmetry, and only ro-vibrational states with odd values of $(K'_a+K'_c)$ are allowed for vibrational states of the B_1 symmetry (here K'_a and K'_c are the quantum numbers of rotational wave functions). In turn, the band (110) is a symmetric one, and, as the consequence, the $\nu_1+\nu_2$ band is a *b*-type band with the selection rules, Ref. [43],

$$\Delta J=0,\ \pm1,\quad \Delta K_a=\text{odd},\quad \Delta K_c=\text{odd}.$$

The assignment of transitions of the $\nu_1+\nu_2$ and $\nu_2+\nu_3$ bands was made on the basis of the ground state combination differences method. As they are necessary for the calculation, ground state rotational parameters and centrifugal distortion coefficients have been take from Ref. [14] (they are reproduced from [14] in column 2 of Table 2). About 1540 and 1390 transitions with $J^{max.}/K_a^{max.}=65/23$ and 67/23 were assigned to the $\nu_1+\nu_2$ and $\nu_2+\nu_3$ bands (the complete list of the assigned transitions together with the corresponding transmittances is presented electronically as Supplementary Material I and Supplementary Material II of this paper; see also statistical information in Table 1). On this basis, we obtained 707 and 740 upper ro-vibrational energies of the (110) and (011) vibrational states (see also statistical information and comparison with earlier study, Ref. [14], in Table 1) out of which small parts are presented as an illustration in Tables 3 and 4 (column 2) together with experimental uncertainties (column 3). We would like to remark that the hot band $\nu_1+\nu_2-\nu_2$ have been used in Ref. [14] for determination of the ro-vibrational energy values of the state (110). The cold band $\nu_1+\nu_2$ which was used in the present paper is considerably weaker than the hot $\nu_1+\nu_2-\nu_2$ band (see, Ref. [14] for details). Nonetheless, we were able to derive more than two times more number of ro-vibrational energy values from the experimental data than it have been made in Ref. [14].

Because the experimentally recorded spectrum shows a high signal-to-noise ratio in this region, an attempt was made to find the hot $\nu_1+2\nu_2-\nu_2$ and $2\nu_2+\nu_3-\nu_2$ bands. We did not succeed to find the $\nu_1+2\nu_2-\nu_2$ band, but were able to assign, for the first time, about 510 transitions ($J^{max.}/K_a^{max.}=44/15$) to the $2\nu_2+\nu_3-\nu_2$ band. The corresponding list of transitions is added to the Supplementary Material II. As before for the (110) and (011) states, the assigned transitions of the $2\nu_2+\nu_3-\nu_2$ band were used to obtain the ro-vibrational energies of the (021) vibrational state (in general, 304 ro-vibrational energies); part of which are presented in Table 5 (column 2) as an illustration.

All the obtained ro-vibrational energies were used then in the weighted least square fit for determination of the parameters of the Effective Hamiltonian in the form of Eqs. (1)–(3). As the total number of spectroscopic parameters for the five vibrational states

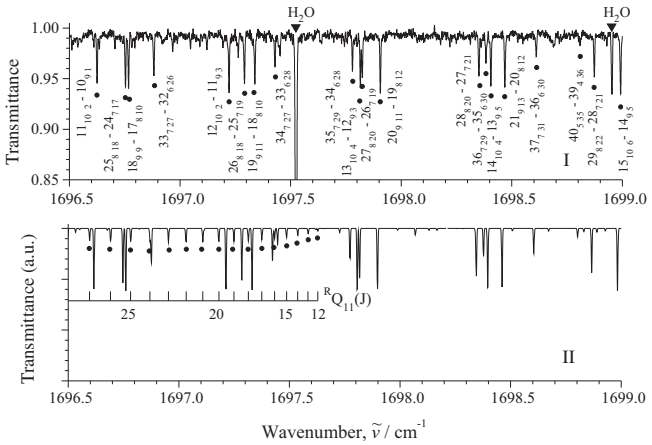

Fig. 3. Small part of the high resolution spectrum (upper trace I) of $^{34}S^{16}O_2$ in the region of the $\nu_1+\nu_2$ band. For the experimental conditions see caption of Fig. 1. The lower trace (II) is the simulated spectrum (see text for details of simulation). Lines assigned to the $\nu_1+\nu_2$ band are marked by dark circles.

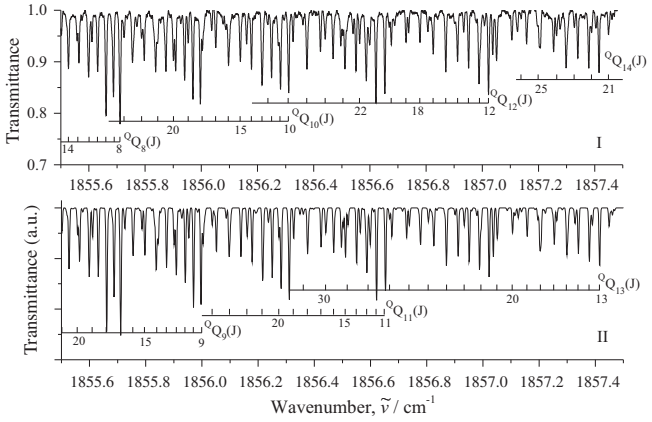

Fig. 4. Small part of the high resolution spectrum (upper trace I) of $^{34}S^{16}O_2$ in the region of the $\nu_2+\nu_3$ band. For the experimental conditions see caption of Fig. 1. The lower trace (II) is the simulated spectrum (see footnote of Fig. 2 for details of simulation). A few sets of transitions assigned to the $\nu_2+\nu_3$ band are marked.

mentioned in Section 3 is large for the fit, most of parameters were constrained to the theoretically estimated values in the fit procedure. In this case, such theoretical estimations have been made in accordance with the scheme discussed in Ref. [25], namely:

(1) The unperturbed vibrational energies of the vibrational states (110), (011) and (030), as well as the main Fermi interaction parameter $^{110\,030}F_0$, have been estimated on the basis of the results and formulas of the Isotopic Substitution theory, Refs. [44,45], and the parameters of the intramolecular potential function from Ref. [15].

(2) Values of the rotational parameters *A*, *B* and *C* of the vibrational states (110) and (011) were estimated on the basis of known values of the equilibrium rotational parameters A_e, B_e and C_e, as well as the α and γ vibration–rotation coefficients from Table 4 of Ref. [23]. To estimate the values of the centrifugal distortion coefficient of these vibrational states we used the following simple relations, which showed a good predictive power in study of analogous XY_2 (C_{2v}) molecules (see Ref. [46]):

$$P^{(v_1v_2v_3)}=P^{(0v_20)}+v_1(P^{(100)}-P^{(000)})+v_3(P^{(001)}-P^{(000)}),\qquad(4)$$

where *P* denotes any of the centrifugal distortion parameters; the values of the initial parameters of the (000), (100), (001) and (010) vibrational states were taken from Ref. [14].

Table 2
Spectroscopic parameters of the (110), (011), (030), (021), and (101) vibrational states of $^{34}S^{16}O_2$ (in cm^{-1}).[a]

Parameter	(000)[b]	(110)[c]	(110)[d]	(110)[b]	(011)[c]	(011)[d]	(011)[b]
1	2	3	4	5	6	7	8
E		1655.15	1654.708372(30)	1654.829004	1855.22	1854.611415(16)	1854.610452
A	1.967733713	2.00642	2.00633098(92)	2.006420332	1.98557	1.98557620(47)	1.985576007
B	0.3441883891	0.34262	0.342623679(80)	0.342625774	0.34311	0.343099725(97)	0.343099540
C	0.2922455227	0.29034	0.29034139(11)	0.2903419697	0.29061	0.290614131(71)	0.2906143287
$\Delta_K \times 10^4$	0.81387956	0.9124	0.914280(79)	0.91420511	0.8897	0.887846(30)	0.88783501
$\Delta_{JK} \times 10^5$	−0.37222039	−0.3745	−0.373571(94)	−0.37283562	−0.4052	−0.406041(49)	−0.4059546
$\Delta_J \times 10^6$	0.21922689	0.2192	0.219099(57)	0.21903597	0.2220	0.222072(43)	0.22210252
$\delta_K \times 10^6$	0.821985	1.0975	1.0946(19)	1.076025	0.9294	0.9411(10)	0.943551
$\delta_J \times 10^7$	0.5746703	0.5758	0.57677(17)	0.5765096	0.5853	0.58565(33)	0.5846747
$H_K \times 10^7$	0.1122874	0.1426	0.14242(24)	0.1426688	0.1358	0.135018(45)	0.1350626
$H_{KJ} \times 10^9$	−0.596544	−0.7645	−0.7538(66)	−0.689952	−0.6132	−0.6128(26)	−0.609127
$H_{JK} \times 10^{11}$	0.1645	0.5213	0.5213	0.43482	0.4243	0.4243	0.43482
$H_J \times 10^{12}$	0.38599	0.4243	0.371(13)	0.3882943	0.3689	0.392(10)	0.3882943
$h_K \times 10^9$	0.55481	0.7099	0.7099	0.70991	0.7099	0.691(11)	0.68694
$h_{JK} \times 10^{13}$	−0.381263781	−0.3813	−0.3813	−0.3812637810	−0.3813	−0.3813	−0.3812637810
$h_J \times 10^{12}$	0.185546	0.1843	0.1843	0.184346	0.1843	0.2066(76)	0.184346
$L_K \times 10^{11}$	−0.209385	−0.300	−0.2942(24)	−0.292804	−0.290	−0.290	−0.292804
$L_{KKJ} \times 10^{12}$	0.11361	0.139	0.132(12)	0.139198	0.139	0.139	0.139198
$L_{JK} \times 10^{15}$	0.727503291	0.728	0.728	0.7275032910	0.728	0.728	0.7275032910
$L_{JJK} \times 10^{17}$	−0.687809164	−0.688	−0.688	−0.6878091640	−0.688	−0.688	−0.6878091640
$L_J \times 10^{18}$	−0.324891428	−0.325	−0.325	−0.3248914280	−0.325	−0.325	−0.3248914280
$P_K \times 10^{15}$	0.29672	0.48	0.48	0.47491	0.48	0.48	0.47491
$P_{KKKJ} \times 10^{16}$	−0.2314	−0.23	−0.23	−0.2314	−0.23	−0.23	−0.2314
$P_{KKJ} \times 10^{17}$	0.13312543	0.13	0.13	0.1331254300	0.13	0.13	0.1331254300

Parameter	(030)[e]	(021)[f]	(021)[d]	(101)[f]	(101)[d]	(101)[g]
1	9	10	11	12	13	14
E	1538.64	2363.54606	2363.546814(23)	2475.7870226	2475.787788(11)	2475.828004
A	2.08707	2.024496	2.02474658(68)	1.94840007	1.94840618(33)	1.948429485
B	0.34437	0.34316	0.34315443(13)	0.341401676	0.341401798(54)	0.341402270
C	0.29062	0.29006	0.29006079(14)	0.289753276	0.289753159(56)	0.289753669
$\Delta_K \times 10^4$	1.0999	0.9882	0.983687(37)	0.812650	0.812650	0.81255487
$\Delta_{JK} \times 10^5$	−0.4223	−0.4226	−0.4226	−0.379854	−0.379854	−0.37974105
$\Delta_J \times 10^6$	0.2205	0.2225	0.2225	0.2211286	0.2211286	0.22117133
$\delta_K \times 10^6$	1.4095	1.1237	1.1237	0.83785	0.83785	0.836844
$\delta_J \times 10^7$	0.5839	0.5887	0.5887	0.580862	0.580862	0.5806223
$H_K \times 10^7$	0.2066	0.1672	0.1672	0.112105	0.112105	0.11202773
$H_{KJ} \times 10^9$	−0.87	−0.7105	−0.7105	−0.5559	−0.5559	−0.544729
$H_{JK} \times 10^{11}$	0.67	0.5395	0.5395	0.2405	0.2405	0.1645
$H_J \times 10^{12}$	0.3860	0.3666	0.3666	0.4038	0.4038	0.41413
$h_K \times 10^9$	0.9	0.8048	0.8048	0.5729	0.5729	0.53402
$h_{JK} \times 10^{13}$	−0.3813	−0.3813	−0.3813	−0.3813	−0.3813	−0.3812637810
$h_J \times 10^{12}$	0.1855	0.1855	0.1855	0.1940	0.1940	0.185546
$L_K \times 10^{11}$	−0.48	−0.386	−0.386	−0.21078	−0.21078	−0.209385
$L_{KKJ} \times 10^{12}$	0.18	0.165	0.165	0.1127	0.1127	0.11361
$L_{JK} \times 10^{15}$	0.728	−0.728	−0.728	0.728	0.728	0.7275032910
$L_{JJK} \times 10^{17}$	−0.688	−0.688	−0.688	−0.688	−0.688	−0.6878091640
$L_J \times 10^{18}$	−0.325	−0.325	−0.325	−0.325	−0.325	−0.3248914280
$P_K \times 10^{15}$	0.82	0.65	0.65	0.30	0.30	0.29672
$P_{KKKJ} \times 10^{16}$	−0.23	−0.23	−0.23	−0.23	−0.23	−0.2314
$P_{KKJ} \times 10^{17}$	0.13	0.13	0.13	0.13	0.13	0.1331254300

[a] Values in parentheses are 1σ statistical confidence intervals (in last digits). Parameters presented without confidence intervals have been constrained to values estimated theoretically (see text for details).
[b] Reproduced from Ref. [14].
[c] Predicted theoretically (see text for details).
[d] Obtained from the fit of experimental ro-vibrational energy values.
[e] Reproduced from Ref. [23] with the exception of the H_K parameter. The H_K parameter was estimated theoretically (see text for details).
[f] Reproduced from Ref. [25] (see text for details).
[g] Reproduced from Ref. [23].

(3) According to the scheme of Ref. [25], all the rotational and centrifugal distortion parameters of the state (030), with the exception of the H_K parameter, were taken from Ref. [23] and are reproduced in column 9 of Table 2. As to the H_K parameter, the following remark should be made. As the visible inspection of the H_K-values for the set of states (000), (010), (020) and (030) shows (see Refs. [14,23]), the value of the H_K parameter of the (030) vibrational state in Ref. [23] is physically unsuitable. For that reason, the initial value of the H_K parameter was estimated with another

Table 3
Small part of experimental ro-vibrational term values for the (110) vibrational state of $^{34}S^{16}O_2$ (in cm^{-1}).[a]

J	K_a	K_c	E	Δ	δ	J	K_a	K_c	E	Δ	δ	J	K_a	K_c	E	Δ	δ	J	K_a	K_c	E	Δ	δ
1			2	3	4	1			2	3	4	1			2	3	4	1			2	3	4
10	0	10	1688.0820	2	0	14	4	10	1748.4822	4	−1	17	11	7	1955.0087	2	0	20	8	12	1895.7724	1	0
10	1	9	1692.6109	3	1	14	5	9	1763.6033	1	0	17	12	6	1993.3518	2	−2	20	9	11	1924.2731	1	1
10	2	8	1696.8731	3	−1	14	6	8	1782.1089	1	−1	17	13	5	2034.9287	4	2	20	10	10	1956.0785	2	0
10	3	7	1704.9477	1	0	14	7	7	1803.9690	4	0	17	14	4	2079.7134	4	−1	20	11	9	1991.1661	3	−1
10	4	6	1716.7131	3	6	14	8	6	1829.1635	1	2	17	15	3	2127.6808	1	0	20	12	8	2029.5131	2	0
10	5	5	1731.8752	2	2	14	10	4	1889.4804	2	−2	17	17	1	2233.0515	2	0	20	13	7	2071.0952		−1
10	6	4	1750.3983	1	1	14	11	3	1924.5643	3	−1	18	0	18	1759.1125	2	−1	20	14	6	2115.8877	1	2
10	7	3	1772.2659	3	1	14	12	2	1962.9029	3	−2	18	1	17	1767.3338	3	−4	20	15	5	2163.8634		0
10	8	2	1797.4627	1	0	14	13	1	2004.4736	3	−2	18	2	16	1772.7666	4	0	20	16	4	2214.9955	4	1
10	9	1	1825.9723	2	1	14	14	0	2049.2518	1	−1	18	3	15	1779.4465	1	0	20	17	3	2269.2544		−2
10	10	0	1857.7761		−2	15	1	15	1728.7733	3	0	18	4	14	1790.5399		−1	20	18	2	2326.6114	2	0
11	1	11	1696.3866	3	2	15	2	14	1737.0939	3	1	18	5	13	1805.5435	4	−1	20	19	1	2387.0349		2
11	2	10	1703.2356	2	−1	15	3	13	1746.2251	3	−1	18	6	12	1824.0049	2	−1	20	20	0	2450.4928	2	1
11	3	9	1711.9055	2	0	15	4	12	1758.0123	2	0	18	7	11	1845.8427	2	0	21	1	21	1794.9318	3	2
11	4	8	1723.6945	1	0	15	5	11	1773.1288	1	1	18	8	10	1871.0260	2	1	21	2	20	1806.1297	3	2
11	5	7	1738.8520	3	1	15	6	10	1791.6269	1	−2	18	9	9	1899.5319	2	1	21	3	19	1816.7015	1	−1
11	6	6	1757.3724	2	−1	15	7	9	1813.4833	1	1	18	10	8	1931.3388		−3	21	4	18	1828.7164	3	1
11	7	5	1779.2390	3	−1	15	8	8	1838.6759	4	1	18	11	7	1966.4264	1	1	21	5	17	1843.7211	3	−2
11	8	4	1804.4358	2	0	15	9	7	1867.1856	2	1	18	12	6	2004.7710	2	1	21	6	16	1862.1292	2	1
11	9	3	1832.9455		−2	15	10	6	1898.9929	3	−1	18	13	5	2046.3491	3	−2	21	7	15	1883.9347	2	0
11	10	2	1864.7506	2	−1	15	11	5	1934.0776	2	−2	18	14	4	2091.1368		1	21	8	14	1909.1004	2	1
11	11	1	1899.8310		0	15	12	4	1972.4183	2	1	18	15	3	2139.1069		0	21	9	13	1937.5970	3	−2
12	0	12	1703.1312	2	1	15	13	3	2013.9908	1	0	18	16	2	2190.2321	1	−1	21	10	12	1969.4010	1	−1
12	1	11	1707.5884	2	1	15	14	2	2058.7711	3	1	18	17	1	2244.4844		2	21	11	11	2004.4886	0	0
12	2	10	1711.8388	1	1	15	15	1	2106.7330	4	0	18	18	0	2301.8328	4	−2	21	12	10	2042.8365	3	0
12	3	9	1719.6155	2	−1	16	0	16	1738.1508	2	0	19	1	19	1770.5455		−1	21	13	9	2084.4206	1	2
12	4	8	1731.3179	3	1	16	1	15	1745.0073	3	0	19	2	18	1780.7121	3	1	21	14	8	2129.2149	1	−1
12	5	7	1746.4653	2	0	16	2	14	1749.8106	2	−1	19	3	17	1790.6942	2	0	21	15	7	2177.1940		1
12	6	6	1764.9822	2	0	16	3	13	1756.8269	1	0	19	4	16	1802.5811	4	3	21	16	6	2228.3297		4
12	7	5	1786.8474	2	2	16	4	12	1768.2177	2	−1	19	5	15	1817.6259	1	0	21	17	5	2282.5924	1	0
12	8	4	1812.0435	2	0	16	5	11	1783.2940	2	0	19	6	14	1836.0738	3	0	21	18	4	2339.9529		−3
12	9	3	1840.5539	3	1	16	6	10	1801.7821	2	−1	19	7	13	1857.9025	2	−1	21	20	2	2463.8439	4	0
12	10	2	1872.3593	1	−2	16	7	9	1823.6332	2	−1	19	8	12	1883.0809	3	−1	21	21	1	2530.3084		−6
12	11	1	1907.4407	1	−3	16	8	8	1848.8235	1	0	19	9	11	1911.5844	2	−2	22	0	22	1807.9584	0	0
12	12	0	1945.7768		0	16	9	7	1877.3324	4	−1	19	10	10	1943.3913	3	1	22	1	21	1818.9617	2	1
13	1	13	1711.4012	2	−4	16	10	6	1909.1402	3	0	19	11	9	1978.4788	2	0	22	2	20	1826.3943	1	−2
13	2	12	1718.9345	3	0	16	11	5	1944.2258	1	−1	19	12	8	2016.8244	2	−2	22	3	19	1832.8547	2	−2
13	3	11	1727.7921	2	−2	16	12	4	1982.5677		0	19	13	7	2058.4050	1	0	22	4	18	1843.0392	3	−3
13	4	10	1739.5745	4	0	16	13	3	2024.1423	3	0	19	14	6	2103.1949		1	22	5	17	1857.7515	2	1
13	5	9	1754.7150	3	−3	16	14	2	2068.9250	3	1	19	15	5	2151.1678		1	22	6	16	1876.1174	1	0
13	6	8	1773.2276	2	0	16	15	1	2116.8898	3	3	19	16	4	2202.2960	3	−3	22	7	15	1897.9078	1	0
13	7	7	1795.0903	2	−1	16	16	0	2168.0089	1	3	19	17	3	2256.5518		−1	22	8	14	1923.0651	1	0
13	8	6	1820.2859	1	0	17	1	17	1748.4909	3	1	19	18	2	2313.9050		4	22	9	13	1951.5576	3	1
13	9	5	1848.7962	2	−1	17	2	16	1757.6931	4	−2	19	19	1	2374.3234		−1	22	10	12	1983.3593	2	1
13	10	4	1880.6026	3	−2	17	3	15	1767.1966	3	0	20	0	20	1782.3802	2	−2	22	11	11	2018.4461		−2
13	11	3	1915.6851	2	−3	17	4	14	1779.0134		2	20	1	19	1791.9986	1	1	22	12	10	2056.7950	3	2
13	12	2	1954.0228		1	17	5	13	1794.0971	3	1	20	2	18	1798.3128	3	1	22	13	9	2098.3803		−1
13	13	1	1995.5915	3	0	17	6	12	1812.5747	2	1	20	3	17	1804.7854	2	−1	22	14	8	2143.1772	3	−2
14	0	14	1719.4906	0	1	17	7	11	1834.4196	1	−1	20	4	16	1815.4711	1	2	22	15	7	2191.1593	2	1
14	1	13	1725.0719	3	−2	17	8	10	1859.6069	2	1	20	5	15	1830.3594	1	−2	22	16	6	2242.2979	3	−1
14	2	12	1729.4901		−1	17	9	9	1888.1146		0	20	6	14	1848.7819	2	0	22	17	5	2296.5656		6
14	3	11	1736.8962		−1	17	10	8	1919.9223	3	1	20	7	13	1870.5998	2	0	22	18	4	2353.9300	1	−2

[a] In Table 3, Δ is the experimental uncertainty of the energy value, equal to one standard error in units of 10^{-4} cm^{-1}; δ is the difference $E^{exp.} - E^{calc.}$, also in units of 10^{-4} cm^{-1}. When the Δ-value is absent, the corresponding energy level was determined from the single transition and was used in the fit with the weight of 1/100.

simple relation which also showed a good predictive power for estimation of parameters of highly excited vibrational states in the XY_2 (C_{2v}) type molecules:

$$P^{(0\,v_2\,0)} = P^{(000)} + v_2 \Delta p_1 + v_2^2 \Delta p_2, \quad (5)$$

where $P^{(000)}$ is the value of a centrifugal distortion coefficient of the ground vibrational state; the coefficients Δp_1 and Δp_2 can be determined from the values of corresponding centrifugal distortion coefficient of the states (010) and (020). Estimated value is also presented in column 9 of Table 2.

(4) The initial values of the vibrational energies E, rotational and centrifugal distortion coefficients of the (021) and (101) vibrational states, and the main Fermi-interaction parameter $^{(101)\ (021)}F_0$ are taken from Ref. [25] where the rotational structure of the state (101) was carefully analyzed, and the state (021) was considered as a "dark" state. Corresponding initial values for two mentioned vibrational states are presented in columns 10 and 12 of Table 2 and in Table 6.

A set of 39 varied parameters obtained from the weighted fit (37 parameters of the diagonal blocks and 2 resonance interaction parameters which are is presented in columns 4, 7, 11 and 13 of Table 2 and in Table 6) reproduces the initial "experimental" ro-vibrational energies with the $d_{rms} = 2.1 \times 10^{-4}$ cm^{-1} for the state (110), $d_{rms} = 2.2 \times 10^{-4}$ cm^{-1} for the state (011), and $d_{rms} = 2.9 \times 10^{-4}$ cm^{-1} for the state (021). One can see that the results obtained for the states (110) and (011) are more than satisfactory. The result is a little bit worse for the (021) vibrational

Table 4
Small part of experimental ro-vibrational term values for the (011) vibrational state of $^{34}S^{16}O_2$ (in cm^{-1}).[a]

J	K_a	K_c	E	Δ	δ	J	K_a	K_c	E	Δ	δ	J	K_a	K_c	E	Δ	δ	J	K_a	K_c	E	Δ	δ
1			2	3	4	1			2	3	4		1		2	3	4	1			2	3	4
10	1	10	1889.5598	0	0	14	5	10	1962.9379	0	0	17	10	7	2117.7331	2	−1	20	8	13	2094.3753	0	0
10	2	9	1896.0511	1	1	14	6	9	1981.2125	1	0	17	11	6	2152.3878	2	0	20	9	12	2122.5236	1	2
10	3	8	1904.5513	1	0	14	7	8	2002.8000	2	0	17	12	5	2190.2606	2	1	20	10	11	2153.9368	1	1
10	4	7	1916.1971	3	0	14	8	7	2027.6812	2	0	17	13	4	2231.3283	2	0	20	11	10	2188.5932	3	0
10	5	6	1931.1703	1	0	14	9	6	2055.8382	4	1	17	14	3	2275.5672	1	1	20	12	9	2226.4705	1	1
10	6	5	1949.4620	1	0	14	10	5	2087.2519	1	0	17	15	2	2322.9513	2	−1	20	13	8	2267.5449	3	0
10	7	4	1971.0570	1	−1	14	11	4	2121.9033	1	1	17	17	0	2427.0482		1	20	14	7	2311.7920	0	0
10	8	3	1995.9405	3	0	14	12	3	2159.7707	1	0	18	1	18	1959.0806	1	0	20	15	6	2359.1863	1	2
10	9	2	2024.0963	1	2	14	13	2	2200.8320		2	18	2	17	1968.7081	1	1	20	16	5	2409.7004	1	2
10	10	1	2055.5065		0	14	14	1	2245.0628		0	18	3	16	1978.3519	1	0	20	17	4	2463.3063		1
11	0	11	1895.6334	2	2	15	0	15	1928.3714	1	0	18	4	15	1990.0549	1	0	20	18	3	2519.9747	2	−1
11	1	10	1899.5940	0	−1	15	1	14	1934.5788		0	18	5	14	2004.9294	1	0	20	19	2	2579.6754		−4
11	2	9	1903.7771	0	0	15	2	13	1939.1277	1	1	18	6	13	2023.1614	0	0	20	20	1	2642.3768		−13
11	3	8	1911.6011	1	2	15	3	12	1946.2221	2	0	18	7	12	2044.7266	1	−1	21	0	21	1994.7677	1	1
11	4	7	1923.1899		1	15	4	11	1957.5660	1	0	18	8	11	2069.5972	1	0	21	1	20	2005.0743	1	0
11	5	6	1938.1559	2	0	15	5	10	1972.4760	1	−1	18	9	10	2097.7504	1	2	21	2	19	2011.9337	0	0
11	6	5	1956.4449	1	−1	15	6	9	1990.7426	1	1	18	10	9	2129.1652	1	2	21	3	18	2018.2918	1	0
11	7	4	1978.0390	2	−1	15	7	8	2012.3263	2	1	18	11	8	2163.8207		2	21	4	17	2028.5619	1	1
11	8	3	2002.9224	1	0	15	8	7	2037.2058	2	0	18	12	7	2201.6948	1	0	21	5	16	2043.1716	1	0
11	9	2	2031.0787	1	1	15	9	6	2065.3624	2	1	18	13	6	2242.7646		−3	21	6	15	2061.3348	1	−1
11	10	1	2062.4901	2	1	15	10	5	2096.7767	1	0	18	14	5	2287.0067	3	2	21	7	14	2082.8673	2	−1
11	11	0	2097.1370		−2	15	11	4	2131.4291	2	−1	18	15	4	2334.3941		1	21	8	13	2107.7203	1	−1
12	1	12	1903.4046		−1	15	12	3	2169.2985		0	18	16	3	2384.9002		−3	21	9	12	2135.8648		0
12	2	11	1910.5277	1	1	15	13	2	2210.3619	1	1	18	17	2	2438.4981		0	21	10	11	2167.2766	1	−1
12	3	10	1919.1817	2	1	15	14	1	2254.5954		1	18	18	1	2495.1581		4	21	11	10	2201.9334		0
12	4	9	1930.8186	1	0	15	15	0	2301.9733		−2	19	0	19	1970.3264	0	0	21	12	9	2239.8119	3	1
12	5	8	1945.7785	1	−1	16	1	16	1938.1760		2	19	1	18	1979.2455	1	1	21	13	8	2280.8883	1	−1
12	6	7	1964.0641	1	0	16	2	15	1946.8766	1	0	19	2	17	1985.0852	1	0	21	14	7	2325.1383	1	0
12	7	6	1985.6567	1	0	16	3	14	1956.0899	1	0	19	3	16	1991.5427	2	−2	21	15	6	2372.5358	1	0
12	8	5	2010.5397	1	−1	16	4	13	1967.7424	1	0	19	4	15	2002.2773	0	0	21	16	5	2423.0537	1	−1
12	9	4	2038.6964	1	0	16	5	12	1982.6530	1	0	19	5	14	2017.0345	1	0	21	17	4	2476.6641	1	0
12	10	3	2070.1086	1	−1	16	6	11	2000.9104	2	1	19	6	13	2035.2457	1	0	21	18	3	2533.3374		−1
12	11	2	2104.7572	1	0	16	7	10	2022.4891	1	−1	19	7	12	2056.8019	1	0	21	19	2	2593.0433		−4
12	12	1	2142.6211	2	−1	16	8	9	2047.3664	2	0	19	8	11	2081.6677	2	0	21	20	1	2655.7515		0
13	0	13	1910.8496	1	0	16	9	8	2075.5229		6	19	9	10	2109.8185	2	0	21	21	0	2721.4289		2
13	1	12	1915.8466	0	0	16	10	7	2106.9371	0	0	19	10	9	2141.2328	2	0	22	1	22	2007.8923	0	0
13	2	11	1920.1111	1	0	16	11	6	2141.5909	1	1	19	11	8	2175.8888	2	−2	22	2	21	2019.5808		1
13	3	10	1927.5934	0	0	16	12	5	2179.4617	2	0	19	12	7	2213.7648	2	0	22	3	20	2030.4176	2	−1
13	4	9	1939.0937	1	0	16	13	4	2220.5272	2	−1	19	13	6	2254.8371	0	0	22	4	19	2042.3923	2	2
13	5	8	1954.0391	1	−1	16	14	3	2264.7635	1	0	19	14	5	2299.0815	1	1	22	5	18	2057.1895	1	1
13	6	7	1972.3199	1	0	16	15	2	2312.1445		−1	19	15	4	2346.4724		2	22	6	17	2075.3401	1	−1
13	7	6	1993.9103	2	0	16	16	1	2362.6442		1	19	16	3	2396.9822	3	−2	22	7	16	2096.8584	1	0
13	8	5	2018.7928	2	2	17	0	17	1948.1959	0	0	19	17	2	2450.5842	3	0	22	8	15	2121.7031	1	0
13	9	4	2046.9495	1	0	17	1	16	1955.7313	1	0	19	18	1	2507.2482		0	22	10	13	2181.2531	1	0
13	10	3	2078.3626		0	17	2	15	1960.7993	0	0	19	19	0	2566.9435		−8	22	11	12	2215.9094	2	−1
13	11	2	2113.0124	1	−1	17	3	14	1967.5265	1	0	20	1	20	1982.3213		1	22	12	11	2253.7889	2	−1
13	12	1	2150.8783	4	0	17	4	13	1978.6207	2	−1	20	2	19	1992.9493	1	0	22	13	10	2294.8677	1	2
13	13	0	2191.9373	0	0	17	5	12	1993.4722	1	0	20	3	18	2003.1341	1	0	22	14	9	2339.1202	0	−1
14	1	14	1919.6140	0	0	17	6	11	2011.7166	1	1	20	4	17	2014.9383	1	−1	22	15	8	2386.5211		−1
14	2	13	1927.4761	0	0	17	7	10	2033.2891	2	−1	20	5	16	2029.7729	1	0	22	16	7	2437.0431	1	−1
14	3	12	1936.3631	3	1	17	8	9	2058.1636	1	1	20	6	15	2047.9698	1	0	22	17	6	2490.6578		−2
14	4	11	1947.9985	1	0	17	9	8	2086.3182	1	0	20	7	14	2069.5154	0	0	22	18	5	2547.3363	1	0

[a] See footnote to Table 3.

state than for the states (110) and (011) because the ro-vibrational energies were obtained from the transitions belonging to the "hot" $2\nu_2 + \nu_3 - \nu_2$ band, which are very weak in comparison with the transitions belonging to the considerably stronger and dense $\nu_2 + \nu_3$ "cold" band (as the consequence, the accuracy in the experimental positions of the "hot" lines is worse). From comparison of theoretically estimated and obtained from the fit values of spectroscopic parameters, one can see that the values obtained from the fit are physically suitable. Also as an illustration of the quality of the result, one can see values of differences $\delta = E^{exp.} - E^{calc.}$ between "experimental" and calculated values of ro-vibrational energies, which are satisfactory, see column 4 of Tables 3–5. We would like to mark that we did not use parameters l_K^v, l_{KJ}^v, l_{JK}^v and l_J^v in the diagonal blocks H^{vv} of the Hamiltonian, Eq. (1) in the present study. The reason is in the following. On the one hand, it is well known from the rotation–vibration theory (see, e.g., Ref. [47]) that the values of spectroscopic parameters of excited vibrational states should be only slightly different from the values of the corresponding parameters of the ground state. On the other hand, we used in the present study parameters of the ground vibrational state from Ref. [14]. Because parameters l_K^v, l_{KJ}^v, l_{JK}^v and l_J^v are absent in Ref. [14], we did not use them in the present study.

It is interesting to compare the values of parameters of the states (110) and (011) obtained in the present study with the parameters of the earlier paper, Ref. [14] (the latter are reproduced from Ref. [14] in columns 5 and 8 of Table 2). One can see that both sets of parameters correlate very well with each other. However, we would like to remark, that the ro-vibrational energies derived in our study from experimental data (about 1450 ro-vibrational

Table 5
Small part of experimental ro-vibrational term values for the (021) vibrational state of $^{34}S^{16}O_2$ (in cm^{-1}).[a]

J	K_a	K_c	E	Δ	δ	J	K_a	K_c	E	Δ	δ	J	K_a	K_c	E	Δ	δ	J	K_a	K_c	E	Δ	δ
1			2	3	4	1			2	3	4	1			2	3	4	1			2	3	4
10	3	8	2413.7716	1	2	15	11	4	2644.8992	1	0	20	9	12	2634.4473		3	25	4	21	2598.5065		0
10	5	6	2441.0156		−1	16	2	15	2455.8597	5	−1	20	10	11	2666.5788	1	3	25	5	20	2612.9289	4	−4
10	6	5	2459.7347	1	1	16	5	12	2492.4585	2	−1	20	11	10	2702.0221		6	25	6	19	2631.3551	1	0
10	10	1	2568.2211	4	1	16	6	11	2511.1436		2	20	12	9	2740.7510		−4	25	8	17	2678.7021		6
11	0	11	2404.4926	1	2	16	8	9	2558.6777	1	1	21	0	21	2503.5051	2	0	25	12	13	2813.7644		−1
11	1	10	2408.5145		1	16	9	8	2587.4807	2	−4	21	1	20	2513.9654	1	−1	26	1	26	2574.6461	1	0
11	2	9	2412.7965	5	−1	16	13	4	2735.7583		−1	21	2	19	2520.9139		2	26	2	25	2588.8156		2
11	3	8	2420.8149		−1	16	14	3	2780.9722		−5	21	3	18	2527.4219	6	1	26	3	24	2601.4919	4	−3
11	4	7	2432.6785		0	16	15	2	2829.3917		0	21	4	17	2537.9662		0	26	4	23	2614.3407	4	−1
11	5	6	2447.9959		0	17	0	17	2456.9964	1	1	21	5	16	2552.9303	3	1	26	5	22	2629.4632	3	2
11	6	5	2466.7123	4	1	17	1	16	2464.6372		−2	21	6	15	2571.5217	4	1	26	6	21	2647.9160	7	−2
11	7	4	2488.8082	2	−2	17	2	15	2469.7913	4	−3	21	7	14	2593.5567	3	−1	26	7	20	2669.8536	2	1
11	9	2	2543.0702	2	−4	17	3	14	2476.6952	1	3	21	8	13	2618.9861	2	1	26	8	19	2695.2260	4	1
11	10	1	2575.1995	7	2	17	5	12	2503.2691		−3	21	9	12	2647.7790		5	26	9	18	2723.9868	1	1
12	1	12	2412.2743		−3	17	6	11	2521.9412	3	−1	21	10	11	2679.9090	3	3	26	10	17	2756.1012		1
12	2	11	2419.5397		0	17	7	10	2544.0157	2	−6	21	14	7	2841.3057	3	2	26	12	15	2830.2741	3	3
12	3	10	2428.3903	2	−2	17	8	9	2569.4660		−5	22	1	22	2516.6131	3	−3	27	0	27	2590.5944	4	−2
12	4	9	2440.3017		3	17	9	8	2598.2691	4	2	22	2	21	2528.5042	2	3	27	1	26	2605.1043		−1
12	5	8	2455.6127	2	0	17	10	7	2630.4018	5	0	22	3	20	2539.5487	7	−1	27	2	25	2616.2012	1	1
12	6	7	2474.3257	1	2	17	14	3	2791.7696		7	22	4	19	2551.7907	3	−2	27	3	24	2623.8697	1	−1
12	7	6	2496.4206	3	4	18	1	18	2467.8727		−2	22	5	18	2566.9380	3	3	27	4	23	2632.8609	5	1
12	8	5	2521.8786	5	−1	18	2	17	2477.6733	4	−3	22	6	17	2585.5159		−3	27	5	22	2646.8434		2
12	9	4	2550.6829	1	2	18	3	16	2487.5178	2	−1	22	7	16	2607.5373		1	27	6	21	2665.1329	5	3
12	10	3	2582.8119		−5	18	4	15	2499.4923	4	0	22	9	14	2661.7466	4	1	27	7	20	2687.0341		0
12	11	2	2618.2461	1	−5	18	5	14	2514.7179	2	1	22	10	13	2693.8749	1	1	27	8	19	2712.3896		4
13	0	13	2419.6933		−4	18	6	13	2533.3767		−6	22	12	11	2768.0504		1	27	12	15	2847.4193		5
13	1	12	2424.7629		2	18	7	12	2555.4455	3	4	22	14	9	2855.2773		−4	28	1	28	2607.1412		2
13	5	8	2463.8671	3	2	18	9	10	2609.6924		0	23	0	23	2530.2221	2	0	28	4	25	2649.4334	4	−1
13	6	7	2482.5750		1	18	10	9	2641.8255	2	3	23	1	22	2542.0699	2	2	28	5	24	2664.5999	3	3
13	7	6	2504.6675	3	0	18	11	8	2677.2670		1	23	2	21	2550.2608		−3	28	7	22	2704.8552		−4
13	9	4	2558.9293	3	−3	18	12	7	2715.9934	4	−2	23	3	20	2556.8814		−3	28	8	21	2730.1922	3	3
13	10	3	2591.0598		−5	18	13	6	2757.9799	4	−3	23	5	18	2581.6307	3	2	28	9	20	2758.9319	4	5
14	1	14	2428.4614		−3	19	0	19	2479.0980	3	2	23	6	17	2600.1538		0	29	0	29	2624.2518	3	−5
14	3	12	2445.5590	2	−1	19	1	18	2488.1452	1	0	23	7	16	2622.1561		−5	29	1	28	2640.0451	2	−2
14	4	11	2457.4678	5	−2	19	2	17	2494.0704		0	23	8	15	2647.5679	3	−1	29	3	26	2661.2952	2	−2
14	6	9	2491.4607	2	0	19	3	16	2500.6924	1	1	23	10	13	2708.4770		1	29	5	24	2683.3995	1	2
14	7	8	2513.5505	4	1	19	4	15	2511.7034	6	1	23	11	12	2743.9200	3	5	29	7	22	2723.3212		7
14	8	7	2539.0078		5	19	5	14	2526.8135	2	1	23	12	11	2782.6528	5	−1	29	8	21	2748.6345	5	2
14	9	6	2567.8112		−4	19	6	13	2545.4523	1	−1	24	1	24	2544.4697	1	0	30	1	30	2641.9534		3
14	11	4	2635.3799	2	−2	19	7	12	2567.5107	3	−5	24	2	23	2557.4827	1	2	30	2	29	2658.4983	1	0
14	12	3	2674.0991		−5	19	8	11	2592.9536	2	6	24	3	22	2569.2930	2	0	30	3	28	2673.1602	3	0
14	13	2	2716.0773		4	19	9	10	2621.7513		−4	24	4	21	2581.7886	2	0	30	4	27	2687.0482	6	0
15	0	15	2437.1958	3	−2	19	10	9	2653.8843	3	3	24	5	20	2596.9096		−2	30	5	26	2702.3191	4	0
15	1	14	2443.4903	3	2	19	11	8	2689.3261	2	−4	24	6	19	2615.4307	1	−1	30	7	24	2742.4263	5	0
15	2	13	2448.1281		0	19	12	7	2728.0551		2	24	7	18	2637.4151		−4	30	8	23	2767.7172		4
15	3	12	2455.4078	2	−2	19	14	5	2815.2666		−2	24	8	17	2662.8155		−1	30	9	22	2796.4290		4
15	4	11	2467.0281	2	3	20	1	20	2491.0798	3	−1	24	9	16	2691.5926	1	2	30	10	21	2828.5155		6
15	5	10	2482.2897		2	20	4	17	2524.3571	1	−1	24	14	11	2885.1283	2	4	31	0	31	2660.2248	1	0
15	6	9	2500.9835		1	20	5	16	2539.5423	3	1	25	0	25	2559.2511		−3	31	1	30	2677.2790	6	−2
15	7	8	2523.0692	4	−2	20	6	15	2558.1664	1	−3	25	1	24	2572.4486	1	1	31	2	29	2691.4036		−4
15	8	7	2548.5240	2	−6	20	7	14	2580.2154		4	25	2	23	2582.0461	3	0	31	3	28	2701.2558		2
15	10	5	2609.4609		1	20	8	13	2605.6511	2	1	25	3	22	2589.0459	1	−1	31	4	27	2709.8610	5	−3

[a] See footnote to Table 3.

Table 6
Resonance interaction parameters for some sets of vibrational states of $^{34}S^{16}O_2$ (in cm^{-1}).[a]

Parameter	Value	Parameter	Value	Parameter	Value
$^{(110)\ (030)}F_0$	3.76				
$^{(101)\ (021)}F_0$	2.17	$^{(101)\ (021)}F_K \times 10^2$	−1.331(56)	$^{(101)\ (021)}F_{xy} \times 10^5$	−0.433(75)

[a] Values in parentheses are 1σ statistical confidence intervals (in last digits). Parameters presented without confidence intervals have been constrained to values estimated theoretically (see text for details).

energies of the states (110) and (011) against 960 ro-vibrational energies obtained in Ref. [14]), are reproduced with our set of parameters with the d_{rms} value about 3.8 and 1.1 times better than the same 1450 energies are reproduced with the parameters from Ref. [14] for the states (110) and (011), respectively (it is the consequence of the fact that, in our study, ro-vibrational energies with higher values of quantum numbers J and K_a than in Ref. [14] were derived from the experimental data). It can be also interesting to compare spectroscopic parameters of the (101) vibrational state (which is mentioned in the present paper because of resonance interaction with the studied (021) state) from column 13 of Table 2 with the parameters of this state from Ref. [23] (the latter are

reproduced in column 14 of Table 2). One can see a good correspondence between parameters from columns 13 and 14, with the exception of the parameter E. The last can be easily understood if to take into account that the value E in column 13 is the unperturbed vibrational energy, but the value E in column 14 is the value of the $(J = 0K_a = 0K_c = 0)$ ro-vibrational level. If one takes into account the value of the Fermi-interaction parameter, ${}^{(101)\ (021)}F_0$, from Table 6, then one can easily obtain the value of the $(J = 0K_a = 0K_c = 0)$ ro-vibrational level in our study, which coincides with high accuracy with the E-value from column 14 of Table 2.

As one more illustration of the correctness of the results obtained in the present study, the simulated spectra of both the $\nu_1 + \nu_2$, and $\nu_2 + \nu_3$ bands were constructed. In our present analysis we followed the analogous analysis of the main, ${}^{32}S^{16}O_2$, species (see, Ref. [16]). Only relative line intensities were calculated, and for the $\nu_2 + \nu_3$ band only one main effective dipole moment parameter was used in the calculation. At the same time, we found that use of only one main effective dipole moment parameter for the $\nu_1 + \nu_2$ band does not allow us to reproduce the form of the band even qualitatively. Only addition of higher-order intensity constants (Herman–Wallis effect) allowed us to correctly simulate spectrum of the $\nu_1 + \nu_2$ band: the same three parameters, as in Ref. [16], i.e., $\varphi_x = 1, \{i\varphi_y, J_z\} = 0.002$, and $\{\varphi_z, iJ_y\} = -0.0012$ have been used.[1] The Doppler profile of lines was used in the calculation. The obtained simulated spectra are presented in the lower traces of Figs. 1–4. One can see more than satisfactory correlations between the experimental and simulated spectra. It can be interesting also to compare the relative ${}^{34}S^{16}O_2/{}^{32}S^{16}O_2$ intensities of the respective $\nu_1 + \nu_2$ and $\nu_2 + \nu_3$ bands in natural abundance. In the present study, we did not measure the line strengths. However, the approximate estimation can be easily made on the analysis of the general formula for line strengths:

$$k_\sigma = \frac{8\pi^3\sigma}{4\pi\epsilon_0 3hc}\left[1 - \exp\left(-\frac{hc\sigma}{kT}\right)\right] N \frac{g_a}{Z(T)} \exp\left(-\frac{E_A}{kT}\right) R_A^B \qquad (6)$$

which is reproduced here from Ref. [48]. It can be easily shown that all values in Eq. (6) are practically not changed under substitution ${}^{34}S^{16}O_2 \leftarrow {}^{32}S^{16}O_2$, with the exception of N which is the number of absorbing molecules per unit volume. This means that the ratio of the line strengths of the same name (as well as of intensities of the bands of the same name) of ${}^{34}S^{16}O_2$ and ${}^{32}S^{16}O_2$ in the natural abundance should be close to 1/24.

5. Conclusion

The high resolution spectrum in the region of the $\nu_1 + \nu_2$ and $\nu_2 + \nu_3$ bands was recorded with a Bruker FS120 HR Fourier transform infrared spectrometer. Considerably higher numbers of transitions, compared to previous studies, were assigned to the $\nu_1 + \nu_2$ and $\nu_2 + \nu_3$ bands. Furthermore, the "hot" $2\nu_2 + \nu_3 - \nu_2$ band was recorded for the first time. Altogether, about 3440 transitions have been assigned in the experimental spectrum to the $\nu_1 + \nu_2$, $\nu_2 + \nu_3$, and $2\nu_2 + \nu_3 - \nu_2$ bands, which enabled us to obtain the values of 1751 ro-vibrational energies of the states (110), (011) and (021) (707 energies with $J^{max.} = 65$ and $K_a^{max.} = 23$ for the state (110); 740 energies with $J^{max.} = 67$ and $K_a^{max.} = 23$ for the state (011); and 304 energies with $J^{max.} = 44$ and $K_a^{max.} = 15$ for the state (021)). The experimental data have been used in the weighted fit and a set of spectroscopic parameters has been obtained which reproduces the initial "experimental" energy values with the d_{rms} values of 2.1×10^{-4} cm^{-1}, 2.2×10^{-4} cm^{-1} and 2.9×10^{-4} cm^{-1} for the states (110), (011) and (021).

[1] We would like to remark that an analogous discussion of the influence of the Herman–Wallis effect on the line strengths was not given by the authors of Ref. [14] since they derived ro-vibrational energies of the (110) vibrational state not from the cold $\nu_1 + \nu_2$ band, but from the hot $\nu_1 + \nu_2 - \nu_2$ band.

Acknowledgments

The work was supported by the project "Leading Russian Research Universities" (Grant FTI-120 of the Tomsk Polytechnic University). Part of the work was supported by the Foundation of the President of the Russian Federation (Grant MK-4872.2014.2) and by the Deutsche Forschungsgemeinschaft (Grants BA 2176/3-2, BA 2176/4-1, BA 2176/4-2, and BA 2176/5-1).

Appendix A. Supplementary material

Supplementary data associated with this article can be found, in the online version, at http://dx.doi.org/10.1016/j.jms.2015.11.003.

References

[1] L.E. Snyder, J.M. Hollis, B.L. Ulich, F.J. Lovas, D.R. Johnson, D. Buhl, Astrophys. J. 198 (1975) 81–84.
[2] L.W. Esposito, J.R. Winick, A.I. Stewart, Geophys. Res. Lett. 6 (1979) 601–604.
[3] S. Self, M.R. RAmpino, J.J. Barbera, J. Volcanol. Geotherm. Res. 11 (1981) 41–60.
[4] R.J. Charlson, T.L. Anderson, R.E. McDuff, in: S.S. Butcher, R.J. Charlson, G.H. Orian, G.V. Wolfe (Eds.), Global Biogeochemical Cycles, Academic, London, 1992, pp. 285–300.
[5] B. Bèzard, C. DeBergh, B. Fegley, J.-P. Maillard, D. Crisp, T. Owen, J.B. Pollack, D. Grinspoon, Geophys. Res. Lett. 20 (1993) 1587–1590.
[6] M.P. McCormic, L.W. Thompson, C.R. Trepte, Nature 373 (1995) 399–404.
[7] R.W. Carlson, W.D. Smythe, R.M.C. Lopes-Gautier, A.G. Davies, L.W. Kamp, J.A. Mosher, L.A. Soderblom, F.E. Leader, R. Mehlman, R.N. Clark, F.P. Fanale, Geophys. Res. Lett. 24 (1997) 2479–2482.
[8] P.J. Wallace, J. Volcanol. Geotherm. Res. 108 (2001) 85–106.
[9] E. Marcq, J.-L. Betraux, F. Montmessin, D. Belyaev, Nat. Geosci. 6 (2013) 25–28.
[10] O.N. Ulenikov, G.A. Onopenko, O.V. Gromova, E.S. Bekhtereva, V.-M. Horneman, J. Quant. Spectrosc. Radiat. Transfer 130 (2013) 220–232.
[11] A. Barbe, C. Secroun, P. Jouve, B. Duterage, N. Monnanteuil, J. Bellet, G. Steenbeckeliers, J. Mol. Spectrosc. 55 (1975) 319–350.
[12] G. Guelachvili, O.V. Naumenko, O.N. Ulenikov, J. Mol. Spectrosc. 125 (1987) 128–139.
[13] G. Guelachvili, O.V. Naumenko, O.N. Ulenikov, J. Mol. Spectrosc. 131 (1988) 400–402.
[14] W.J. Lafferty, J.-M. Flaud, R.L. Sams, ElH.A. Ngom, J. Mol. Spectrosc. 252 (2008) 72–76.
[15] O.N. Ulenikov, E.S. Bekhtereva, S. Alanko, V.M. Horneman, O.V. Gromova, C. Leroy, J. Mol. Spectrosc. 257 (2009) 137–156.
[16] O.N. Ulenikov, O.V. Gromova, E.S. Bekhtereva, I.B. Bolotova, C. Leroy, V.M. Horneman, S. Alanko, J. Quant. Spectrosc. Radiat. Transfer 112 (2011) 486–512.
[17] R. Van Riet, Ann. Soc. Sci. Bruxelles 78 (1964) 237–267.
[18] Y. Morino, Y. Kukuchi, S. Saito, E. Hirota, J. Mol. Spectrosc. 13 (1964) 95–118.
[19] A. Barbe, C. Secroun, P. Jouve, B. Duterage, N. Monnanteuil, J. Bellet. Mol. Phys. 34 (1977) 127–130.
[20] A.S. Pine, G. Dresselhaus, B. Palm, R.W. Davies, S.A. Clough, J. Mol. Spectrosc. 67 (1977) 386–415.
[21] S.P. Belov, M.Y. Tretyakov, I.N. Kozin, E. Klisch, G. Winnewisser, W.J. Lafferty, J.-M. Flaud, J. Mol. Spectrosc. 191 (1998) 17–27.
[22] J. Henningsen, A. Barbe, M.-R. De Backer-Barilly, J. Quant. Spectrosc. Radiat. Transfer 109 (2008) 2491–2510.
[23] W.J. Lafferty, J.-M. Flaud, ElH.A. Ngom, R.L. Sams, J. Mol. Spectrosc. 253 (2009) 51–54.
[24] J.-M. Flaud, W.J. Lafferty, R.L. Sams, J. Quant. Spectrosc. Radiat. Transfer 110 (2009) 669–674.
[25] O.N. Ulenikov, E.S. Bekhtereva, O.V. Gromova, T. Buttersack, C. Sydow, S. Bauerecker, J. Quant. Spectrosc. Radiat. Transfer 169 (2016) 49–57.
[26] O.N. Ulenikov, O.V. Gromova, E.S. Bekhtereva, Yu.V. Krivchikova, E.A. Sklyarova, T. Buttersack, C. Sydow, S. Bauerecker, J. Mol. Spectrosc. 318 (2015) 26–33.
[27] W.J. Lafferty, A.S. Pine, G. Hilpert, R.L. Sams, J.-M. Flaud, J. Mol. Spectrosc. 176 (1996) 280–286.
[28] O.N. Ulenikov, E.S. Bekhtereva, Yu.V. Krivchikova, Yu.B. Morzhikova, T. Buttersack, C. Sydow, S. Bauerecker, J. Quant. Spectrosc. Radiat. Transfer 166 (2015) 13–22.
[29] O.N. Ulenikov, E.S. Bekhtereva, Yu.V. Krivchikova, V.A. Zamotaeva, T. Buttersack, C. Sydow, S. Bauerecker, J. Quant. Spectrosc. Radiat. Transfer 168 (2016) 29–39.
[30] L.S. Rothman, I.E. Gordon, A. Barbe, D.C. Benner, P.F. Bernath, M. Birk, et al., J. Quant. Spectrosc. Radiat. Transfer 110 (2009) 533–572.

[31] O.N. Ulenikov, E.S. Bekhtereva, V.M. Horneman, S. Alanko, O.V. Gromova, J. Mol. Spectrosc. 255 (2009) 111–121.
[32] A.D. Bykov, Yu.S. Makushkin, O.N. Ulenikov, J. Mol. Spectrosc. 99 (1983) 221–227.
[33] O.N. Ulenikov, G.A. Ushakova, J. Mol. Spectrosc. 117 (1986) 195–205.
[34] J.-J. Zheng, O.N. Ulenikov, G.A. Onopenko, E.S. Bekhtereva, S.-G. He, X.-H. Wang, S.-M. Hu, H. Lin, Q.-S. Zhu, Mol. Phys. 99 (2001) 931–937.
[35] J.K.G. Watson, J. Chem. Phys. 46 (1967) 1935–1949.
[36] O.N. Ulenikov, H. Bürger, W. Jerzembeck, G.A. Onopenko, E.S. Bekhtereva, O.L. Petrunina, J. Mol. Struct. 599 (2001) 225–237.
[37] O.N. Ulenikov, J. Mol. Spectrosc. 119 (1986) 144–152.
[38] X.-H. Wang, O.N. Ulenikov, G.A. Onopenko, E.S. Bekhtereva, S.-G. He, S.-M. Hu, H. Lin, Q.-S. Zhu, J. Mol. Spectrosc. 200 (2000) 25–33.
[39] S.-M. Hu, O.N. Ulenikov, G.A. Onopenko, E.S. Bekhtereva, S.-G. He, X.-H. Wang, H. Lin, Q.-S. Zhu, J. Mol. Spectrosc. 203 (2000) 228–234.
[40] Z.-Y. Zhou, X.-G. Wang, Z.-P. Zhou, O.N. Ulenikov, G.A. Onopenko, Q.-S. Zhu, Mol. Phys. 92 (1997) 1073–1082.
[41] O.N. Ulenikov, E.S. Bekhtereva, S.V. Grebneva, H. Hollenstein, M. Quack, Mol. Phys. 104 (2006) 3371–3386.
[42] O.N. Ulenikov, E.S. Bekhtereva, O.V. Gromova, S. Alanko, V.M. Horneman, C. Leroy, Molec. Phys. 108 (2010) 1253–1261.
[43] O.N. Ulenikov, E.S. Bekhtereva, S.V. Grebneva, H. Hollenstein, M. Quack, Phys. Chem. Chem. Phys. 7 (2005) 1142–1150.
[44] A.D. Bykov, Yu.S. Makushkin, O.N. Ulenikov, J. Mol. Spectrosc. 85 (1981) 462–479.
[45] A.D. Bykov, Yu.S. Makushkin, O.N. Ulenikov, J. Mol. Spectrosc. 93 (1982) 46–54.
[46] O.N. Ulenikov, S.-M. Hu, E.S. Bekhtereva, G.A. Onopenko, S.-G. He, X.-H. Wang, et al., J. Mol. Spectrosc. 210 (2001) 18–27.
[47] D. Papousek, M.R. Aliev, Molecular Vibrational–Rotational Spectra, Elsevier, Amsterdam, 1982.
[48] J.-M. Flaud, C. Camy-Peyret, J. Mol. Spectrosc. 55 (1975) 278–310.